Egypt. J. Chem. **Vol. 66**, No. 9. pp. 321 - 332 (2023)

Egyptian Journal of Chemistry

http://ejchem.journals.ekb.eg/

Proposed Novel Genetic And Epigenetic Effects of Betulinic Acid Against Breast Cancer Cells: *In Silico* and *In Vitro* Study.

Hewida H. Fadel,[a]* Esraa El-Wakeel, , Hanaa Donia,[b] Mohamed Abd El-Rahman,[c] Hadeer Adel EL-Esseily,[d] Tarek El Sewedy[e]

[a]*Department of Medical Laboratory Technology, Faculty of Allied Medical Science, Pharos University, Alexandria, Egypt.*

[b]*Department of Clinical and chemical pathology, Faculty of Medicine, Alexandria University, Egypt*

[c]*Department of Clinical and chemical pathology, Hospital of Military Medical Academy, Alexandria, Egypt.*

[d]*Department of health Care, Faculty of Computer and Data Science, Alexandria University, Alexandria, Egypt.*

[e]*Department of Applied Medical Chemistry, Medical Research Institute, Alexandria University, Egypt.*

Abstract

Estrogen receptor (ER) and the Piwi-Like Protein 1 (PIWIL1) oncogene alter the expression and methylation of oncogenes and tumor suppressor genes. Potential cross-talk between ER and the methylated-DNA binding protein, Kaiso, and its downstream genes c-Myc and CDKN2A remains unexplored. Dual targeting of ER and PIWIL1 might be an excellent therapeutic approach. We aimed to explore natural drug that exerted anti-carcinogenicity in MCF-7 and MDA-MBA-231 with high efficacy and its mode of action. Initially, we used *in silico* molecular docking to identify potential blockers for ER and PIWIL1 among seven natural drugs previously reported anticancer compounds. The best candidate was tested *in vitro* for its influence on KAISO expression by RT-PCR, promoter methylation of c-Myc and CDKN2A by methylation-specific PCR, cell cycle and apoptosis by flowcytometry, and cytotoxicity by MTT assay in the ER(+) MCF-7, and ER(−) MDA-231-MB breast cancer cell lines. Betulinic acid (BA) docked ER-α and PIWIL1 perfectly at critical amino acids with the lowest binding energy. Moreover, ER and PIWIL1 docked Kaiso with root mean square deviation = 5.05 Å and 4.75 Å, respectively, at the critical amino acid Y537. Experimentally, BA caused a dose-dependent cytotoxicity in both MCF-7 and MDA-MB-231 cells (IC_{50}= 21.3 ± 0.05 and 100 ± 0.34 µM), respectively. BA caused a significant dose-dependent G0/G1 cell cycle arrest, apoptosis induction, and upregulated Kaiso expression coincided with increased methylation of c-Myc and demethylation of CDKN2A promoter regions. We are proposing a novel anticancer mechanism of action for BA via potential inhibition of Estrogen-ER-α and PIWIL1 signaling, modulation of KAISO expression and selective alterations in methylation state of c-Myc and CDKN2A key cancer-associated genes.

Keywords: Betulinic acid; breast cancer; Kaiso; c-Myc; Estrogen receptor; PIWIL1.

1. Introduction

Worldwide, breast cancer (BC) is the most common type of cancer among women. Although many adjuvant therapies have been approved and treatment protocols have advanced significantly, BC rates remain the highest in high-income countries [1]. The development of BC involves both genetic and epigenetic alterations. Several epigenetic alterations that contribute to drug resistance in BC were identified, and epigenetic-based therapies may be used to treat these abnormalities [2]. Hormone-dependent estrogen receptor-positive ER (+) breast cancer accounts for over 75% of all breast cancers in women [3]. Estrogen receptors alpha (ERα) and beta

*Corresponding author e-mail: hewida.fadel@pua.edu.eg.; (H. H. Fadel).
Received date 2022-12-02; revised date 2023-01-15; accepted date 2023-01-16
DOI: 10.21608/EJCHEM.2023.178370.7259

(ERβ) are nuclear transcription factors that regulate several physiological processes in different systems, including the reproductive, skeletal, cardiovascular, and nervous systems. While ERβ levels are reduced in tumor cells, ERα, on the contrary, is abundantly expressed in the majority of breast malignancies and has been associated with prognosis and response to hormonal therapy [4]. The identification of compounds possessing ERα specificity still constitutes a major challenge, and selective estrogen receptor modulators that target and block Estrogen-ERα signaling such as Tamoxifen, an ERα antagonist are being used in the adjuvant treatment of hormone-sensitive cancers [5]. However, Tamoxifen resistance and side effects were reported during treatment [6].

PIWI-like protein 1 (PIWIL1) is a PIWI RNA-binding protein that plays an essential role in RNA silencing, proliferation and epigenetic regulation, stem cell maintenance, genomic integrity, epithelial - mesenchymal transition (EMT) and metastasis, and PIWIL1 was classified as an upregulated oncogene that is overexpressed in different cancers including gastric cancer, lung cancer and breast cancer [7]. Several studies have shown that Estrogen-mediated signalling could regulate the expression of the PIWI family, but the molecular basis for such correlation is yet unknown. Moreover, the identification or investigation of the effect of potential inhibitors to PIWIL1 on cancer progression is still unreported [8-10].

Transcription factor Kaiso (POZ/BTB family protein) is a major member of the Zinc finger protein family of methyl-CpG-binding proteins (MBPs), and has been shown to modulate normal gene expression and tumorigenesis by regulating the transcription of certain genes involved in cell division, apoptosis, migration, and invasion [11]. The role of Kaiso in cancer remains largely controversial even within the same tissue type since it was reported to be implicated in tumor-cell proliferation either through pro-oncogenic [12] or tumor-suppressive roles [13] via binding to both methylated and non-methylated DNA motifs [14]. Kaiso modulates the gene expression, epigenetic status, and actions of two nuclear proteins that participate in the proliferation, differentiation, senescence, and apoptosis of cells, c-Myc proto-oncogene [15] and $p16^{Ink4a}$ protein encoded by the cyclin-dependent kinase inhibitor 2A (CDKN2A) tumor suppressor gene [16], dysregulation of these two-cell cycle-controlling genes is frequently associated with various types of human cancer [17]. Notably, Kaplun D et al, have recently reported that Kaiso could modulate the methylation status and therefore, the activity of ER binding site [18].

Many dietary substances have significant anti-tumor effects by reverting epigenetic changes associated with oncogene activation and tumor suppressor gene inactivation [19]. The antitumor effect of natural substances such as Acacetin [20], Coumarin [21], Tryptanthrin [22], Arteminisin [23], Ferulic acid [24], Calcitriol [25], and Betulinic acid (BA) [26] was previously reported. BA is a natural pentacyclic triterpene isolated from birch trees, it has a potential against many diseases such as viral infection, inflammation, and different types of cancers [27].

Although the efficacy of BA in the treatment of cancer cells might be investigated before, however, novel molecular targets and potential epigenetic modulatory actions remain unexplored.

This study aims to screen several natural plant-derived anticancer compounds to identify potential, and the most potent inhibitor for ERα and PIWIL1 by *in silico* virtual molecular docking study. Then, an *in vitro* study on the ER(+) MCF-7, and ER(−) MDA-231-MB BC cell lines was performed to investigate the effect of the best-selected candidate on KAISO mRNA expression, the methylation status of c-Myc and CDKN2A genes, cell cycle progression, apoptosis induction, and cytotoxicity.

2. Materials and Methods

2.1. In Silico Study

2.1.1. Drugs Docking

Docking of Acacetin, Coumarin, Tryptanthrin, Arteminisin, Ferulic acid, Calcitriol, and Betulinic acid to both ERα (PDB DOI: 10.2210/pdb3ERT/pdb) and PIWIL1 PAZ domain (PDB DOI: 10.2210/ pdb2L5C/pdb) was done using ChemSketch, Avogadro energy for drug optimization, Spdbv for energy optimization of 3ERT and PIWIL1, discovery studio 2021 for visualization tool of ligand-receptor, iGemodock for molecular docking.

2.1.2. Molecular Docking

ClusPro was used for molecular docking to evaluate the protein-protein interactions between 3ERT, PIWIL1, Kaiso (PDB DOI: 10.2210/ pdb6DF5/pdb) which consists of one chain (A;134 a.a.) and two nucleotides polymers D and E, each consists of 18 nucleotides (nt), CDKN2A 1A5E (PDB DOI: 10.2210/pdb1A5E/pdb) and c-Myc 7C36 (PDB DOI: 10.2210/pdb7C36/pdb). In addition, Pymol was used to visualize the protein-protein interaction and Prodigy provided us with the binding affinity (ΔG) and the dissociation constant (K_d) values.

2.2. In vitro study

2.2.1. Chemical reagents

All reagents and chemicals were of analytical grade and purchased from Sigma-Aldrich (St. Louis, MO, USA), Betulinic acid (BA) powder was purchased from Sigma Aldrich, USA (Cat # 472-15-1), then was dissolved in DMSO from Sigma Aldrich (Cat #67-68-5). Betulinic acid was dissolved in 0.1% DMSO.

2.2.2. Cell Culture and BA treatment

The study was conducted on the MCF-7 and MDA-MB-231 human breast cancer cell lines. Cells were obtained from the American Type Culture Collection (ATCC), Rockville, MD, USA, and cultured according to standard mammalian tissue culture protocols and sterile techniques. In all treatment protocols, both cell lines were either treated with 0.1% DMSO (control) or with the predetermined low dose of 10% IC_{50} or high dose IC_{50} of BA for 48 hours before the respective analysis. All experiments were independently repeated at least 3 times.

2.2.3. Cytotoxicity measurement assay (MTT assay)

The 3-(4,5-dimethylthiazol-2-yl)-2,5-diphenyl-2H-tetrazolium bromide (MTT) colorimetric assay was performed to examine the effect of 48 hours of BA treatment on the cell viability against the MDA-MB-231 and MCF-7 cells. The IC_{50} values for BA were calculated by nonlinear regression of the dose-response curve for both cell lines as previously described [28].

2.2.4. Analysis of cell cycle by Flow cytometry

MCF-7 and MDA-MB-231 cells (1×10^6 cells/ml) were seeded in 6-well plates and incubated overnight to reach exponential growth before the cells were treated with BA (IC_{50} and 10% of IC_{50}) for 48 hours. After treatment, control and treated cells were collected by trypsiniztion and washed twice with cold PBS, and fixed in 70% ethanol. Immediately before the analysis, cells were washed with PBS and stained with a solution containing 400 µl PI for 30 min at 4 ℃ and 100 µl RNase A for 30 min at 37 ℃. The distribution of cells in the cell cycle was measured at 488 nm by BD FACSCalibur™ with proper settings.

2.2.5. Apoptosis analysis by Flow cytometry using Annexin V-FITC and PI staining.

Analysis of the cell death mechanism by flow cytometry was performed by double staining of MDA-MB-231 and MCF-7 cells by Annexin V-FITC and PI as described [29]. In brief, after exposure to BA for 48 hours, cells were trypsinized and collected, and rinsed in cold PBS. After washing, 1 × 106 cells were stained with AnnexinV-FITC and PI in the dark for 15 min at room temperature before the cells were pelleted and analyzed using BD FACSCalibur™.

2.2.6. RNA extraction, cDNA synthesis and quantitative real-time PCR

All reagents and kits for RNA extraction, cDNA synthesis, and RT- PCR were purchased from (Thermo Fisher Scientific, Waltham, MA, USA Scientific) and experiments were performed according to the manufacturer's instructions. In brief, after each treatment, total RNA was isolated from MCF-7 and MDA-MB-231 cells using the Gene JET RNA Purification Kit. The RNA concentration and purity were assessed by nanodrop spectrophotometer at 260/280 and 260/230 nm and the ratio were ~ 2.0 - 2.2 indicating a high-purity RNA. The extracted mRNA was reverse-transcribed to generate first-strand cDNA using the MultiScribe Reverse Transcriptase. Finally, real-time PCR was performed using the TaqMan Universal Master Mix II and the TaqMan KAISO Gene Expression Assay kit. The PCR amplification conditions consisted of 10 min at

95 ℃ followed by 40 cycles of denaturation at 95 ℃ for 15 s, annealing for 15 s at 60 ℃ and extension for 15 s at 72 ℃. Relative expression for the KAISO gene was calculated by the comparative 2-ΔΔCt method using the endogenous β-actin as a housekeeping gene.

2.2.7. Analysis of Methylation status of c-Myc and CDKN2A promoter by methylation-specific PCR (MSP)

Genomic DNA was isolated from control and BA-treated MCF-7 and MDA-MB-231 cells using the QIAamp DNA Mini Kit (QIAGEN, MD, USA) following to manufacturer's instructions. The methylation status of the CpG islands in the promoter regions of c-Myc and CDKN2A were determined by bisulfite modification that was performed using the EpiTect Fast Bisulfite Conversion Kit (QIAGEN, MD, USA) followed by MSP-PCR that was carried out using specific primers for methylated (M) and unmethylated (U) c-Myc and CDKN2A genes, 2 µg of DNA were used/reaction. The Methprimer [30] software (http://www.urogene.org/cgi-bin/ meth primer2/MethPrimer.cgi), was used for the identification of the potential CG island promoter-rich regions and the MSP primer design for both genes. Primer sequence, product size and accession number for both c-Myc and CDKN2A genes are illustrated in Table 1. The PCR conditions were as follows: 5 min at 94 ℃ followed by 40 cycles of: denaturation at 94 ℃ for 30 s, annealing for 30 s at 60 ℃ and extension for 30 s at 72 ℃. Finally, 10 µl of the final PCR products were separated by electrophoresis on a 1.0 % agarose gel at 100 mA for 45 min and then visualized under UV illumination. The AccuBand™ 50 bp DNA Ladder II from (SMOBIO, Inc., Hsinchu, Taiwan) was used as a molecular weight marker.

2.2.8. Statistical analysis

Data were analyzed using IBM SPSS version 20. Statistical tests, one-way ANOVA, and Tukey post hoc were conducted for pairwise comparisons. Data are represented as mean ± SD of at least three independent experiments. A P-value less than 0.05 was considered statistically significant.

3. Results

3.1. Drug docking

Seven selected natural compounds were docked against 3ERT and PIWIL1. As shown in Table (2) and Figure (1), BA showed the most favourable conformation, as represented by the lowest free energy of binding (-85.59 Kcal/Mol) with PIWIL1. BA formed hydrogen bonds with Tyr 526 with a distance of 2.71 Å in 3ERT and Asp 320, Arg370, and Gly378 in PIWIL1 with distances 4.42 Å, 5.73 Å, and 3.65 Å, respectively. None of the screened products formed hydrogen bonds with the active binding sites in 3ERT (515-535) except calcitriol form one hydrogen bond with Arg515 with a distance of 5.40 Å which was longer than that with BA, in addition to two hydrogen bonds which were formed with Asn455 and Ser456 with distance 3.96 Å and 3.87 Å in 3ERT. The binding energy between BA and 3ERT (-79.14 Kcal/ Mol) was lower than that with Calcitriol (-78.08 Kcal/ Mol.). Moreover, none of the screened natural products formed HB with one of the active binding sites of PIWIL1 (369-378). We found that kaiso binds to PIWIL1 (match align score 11.000, RMSD = 0.473 Å). Kaiso binds to ER (3ert) and showed a match align score of 18.000 and RMSD = 5.036 (3 to 3 atoms).

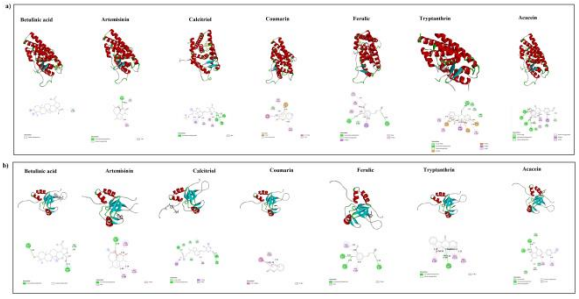

Fig.1. 3D images representing in silico natural compounds docking against (a) estrogen receptor (3ERT) and (b) PIWIL1 (2L5C) with Betulinic acid Artemisinin, Calcitriol, Courmin, Ferulic acid, Tryptanthrin and Acacetin.

3.2. Molecular Docking

Molecular docking data showed that KAISO can bind to two crucial Tyrosine residues (Y526 and Y537), Methionine (Met421), and cysteine (C530) of 3ERT, and many residues within the loop extended from 369 to 378 including R369 R370 P372 of PIWIL-1 with high efficiently as shown in Table (3) and Figure 2.

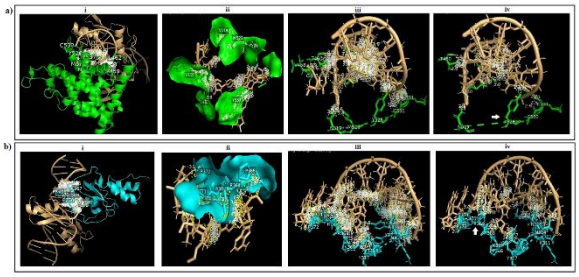

Fig.2. 3D images representing in silico molecular docking for protein-protein interaction between Kaiso protein (6DFB) in light brown and a): estrogen receptor (3ERT) in green, b): PIWIL1 (2L5C) in cyan. (i) The PPI between the whole proteins structure, (ii) surface model of binding site, (iii) PPI between the studied proteins using distance cut-off 4.0 Å and (iv) PPI between the studied proteins using distance cut-off 3.5 Å.

3.3. *Cytotoxic effect of Betulinic acid on MCF-7 and MDA-MB231 cells*

The MTT assay was used to evaluate cell viability after treatment of MCF-7 and MDA-MB231 cells with various BA concentrations. BA caused significant dose-dependent cytotoxicity in treated cells, the calculated IC_{50} against MCF-7 and MDA-MB-231 were 21.3 ±0.05 µM and 100±0.34 µM, respectively, Figure 3.

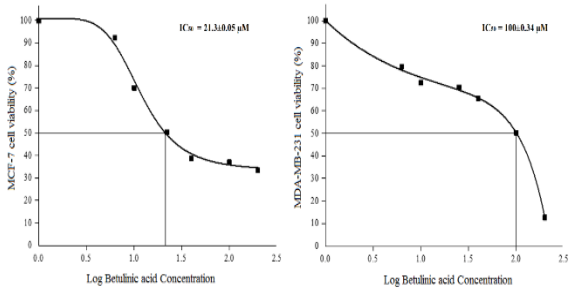

Fig.3. Growth inhibitory curves for the calculation of IC50 for BA in MCF-7 and MDA-MB-231 cell lines. Cells were exposed to different concentrations of BA for 48 hours, and cell viability was determined by MTT assay. Data are expressed as mean ± SD (n = 3).

3.4. *Morphological changes in MCF-7 and MDA-MB231 cells treated with Betulinic acid*

Treatment with BA resulted in a dose-dependent morphological alteration in both MCF-7 and MDA-MB-231 cells that are characteristic of unhealthy dying cells where they had lower proliferation rate and confluency, Figure 4.

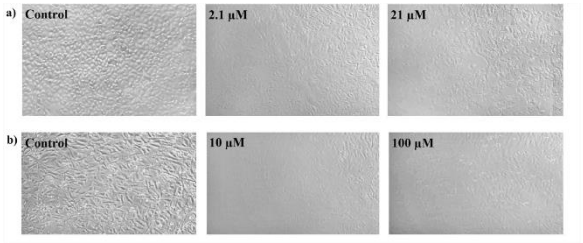

Fig.4. Representative images showing morphological changes in (a) MCF-7 and (b) MDA-MB-231 cell lines after treatment with different concentration of Betulinic acid. Cells were examined and photographed under inverted phase contrast microscope, 100x magnification.

3.5. *Betulinic acid arrests cell cycle in MCF-7 and MDA-MB-231 cells*

Cell cycle phase distribution was analyzed by flow cytometry for control and after treatment of MCF-7 and MDA-MB-231 cells with 10% IC_{50} and IC_{50} BA for 48 hours, Figure 5. Treatment of MCF-7 cells with BA induced a dose-dependent G0/G1 cell cycle arrest; the percentage of cells in the G0/G1 phase was 43.88±0.98% in control and 58.07±0.63% in IC_{50} (20 µM) treated cells. Similarly, treatment of MDA-MB-231 cells with BA induced a significant G0/G1 cell cycle arrest using IC_{50} (100 µM) dose that resulted in accumulation of cells in G0/G1 (57.83±0.58%) compared to control cells (41.52±0.93%). Moreover, Sub-G1 cells were significantly ($P<0.05$) increased by treatment with IC_{50} BA in MCF-7 (5.34±0.56%) and MDA-MB-231 cells (12.65±0.23%), compared to control MCF-7 and MDA-MB-231 cells (1.12% and 4.35±0.45%), respectively.

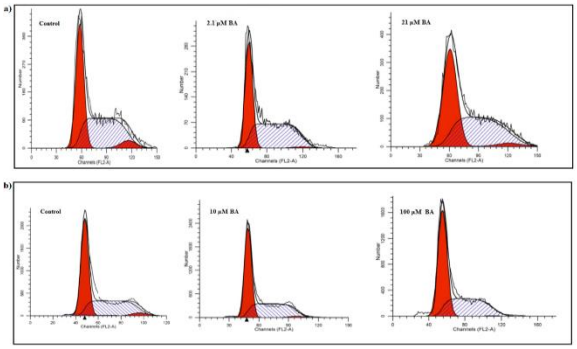

Fig.5. Assessment of cell cycle phase distribution by flow cytometry for (A) MCF-7 and (B) MDA-MB-231 cells lines. Cells were either 0.1% DMSO treated (control) or treated with 10% IC50 and IC50 of BA for 48 hours or cell cycle phases were analyzed by flowcytometry.

3.6. *Effect of BA treatment on cell death mechanism*

Cell death mechanism involved in the BA cytotoxic action was investigated after double staining of cells by Annexin V-FITC and PI as

prescribed earlier in materials & methods and analyzed by flow cytometry. Stained cells appeared as follows: viable (Annexin V-/PI-), early apoptotic (Annexin V+/PI-), late apoptotic (Annexin V+/PI+), and necrotic cells (Annexin V-/PI+), Figure 6.

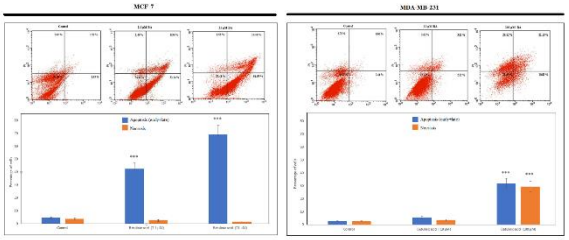

Fig.6. Assessment of apoptosis and necrosis in MCF-7 and MDA-MB-321 after BA treatment for 48 hours. The upper panel shows cells stained with annexin V-FITC and PI, analyzed by flowcytometry. In lower panels, apoptotic (early + late) and necrotic cells are plotted and represented as percentage of total events. Data are expressed as mean ± standard deviation; n=3, (***p < 0.001) significantly different compared to control.

In MCF-7 cells, treatment with 2.1 µM or 21 µM of BA caused a highly significant ($p< 0.001$) dose dependent increase in the percentage of cells undergoing early+late apoptosis (42.33±4.67% and 68.99±7.07%) compared to control cells (4.55±0.35%), respectively. No significant change in necrotic cells was observed in any of the BA-treated MCF-7 cells compared to the control.

Notably, treatment of MDA-MB-231 cells with BA caused a dose-dependent significant increase in both apoptotic and necrotic cells. Only treatment of MDA-MB-231 cells with the high BA dose (100 µM), resulted in a significant ($p< 0.001$) increase in total apoptotic cells (31.96±3.9%), compared to control cells (2.55±0.4%). Simultaneously, the same treatment resulted in a significant increase in the percentage of necrotic cells compared to control (29.56±4.12% and 2.67±0.32%), respectively. Figure 6.

3.7. *Betulinic acid upregulates Kaiso expression in MCF-7 and MDA-MB-231 cells*

MCF-7 and MDA-MB-231 cells were treated with the predetermined 10% IC_{50} or IC_{50} concentration of BA for 48 hours, and relative Kaiso gene expression was measured by real-time PCR (Figure 7). A statistically non-significant increase in Kaiso expression was observed in MCF-7 ($p=0.060$) and MDA-MB- 231 cells ($P = 0.843$) treated with 10% IC_{50} of BA, compared to control cells. On the other hand, treatment of cells with the higher IC_{50} dose caused a statistically significant increase in Kaiso expression by 14.27 fold ($p<0.001$) in MCF-7 and 9.07-fold ($p=0.004$) in MDA-MB-231, compared to control and cells treated with 10% IC_{50} (BA). Therefore, collectively, BA treatment has caused a dose-dependent increase in Kaiso gene expression in both MCF-7 and MDA-MB-231 cells.

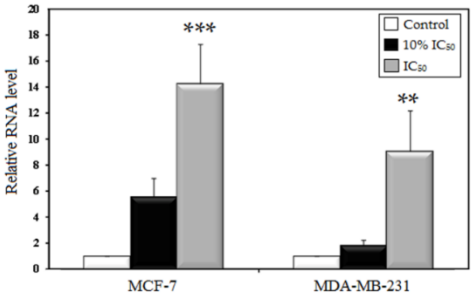

Fig.7. Relative expression levels of Kaiso gene in MCF-7 and MDA-MB231 cells treated with 10% IC50 and IC50 of BA for 48 hours. Real-time PCR reactions were performed, data are represented as mean of three replicates ± standard deviation (**p < 0.005 and *** p < 0.001 compared to control).

3.8. *Promoter methylation analysis for CDKN2A and c-Myc genes*

The potential effect of BA treatment on the promoter methylation status of CDKN2A and c-Myc genes was investigated by MS-PCR analysis, Figure 8. Data reveals that treatment of MCF-7 and MDA-MB231 cells with BA caused a dose-dependent increase in the unmethylation of the CDKN2A gene compared to control in both cell lines. On the other hand, BA treatment increased the methylation of the c-Myc gene promoter in a dose-dependent manner in both models of cell lines tested.

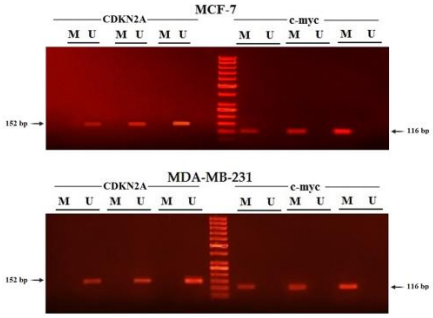

Fig.8. Representative Agarose gel electrophoresis for MS-PCR analysis showing the promoter methylation status for CDKN2A and c-Myc genes in MCF-7 and MDA-MB-231 cells in control and after treatment with 10% IC50 and IC50 of (BA) for 48 hours then analysis by MS-PCR followed by gel electrophoresis with a 50 bp DNA ladder. Amplification with the (M) primer reveals methylation, amplification with the (U) primer reveals de-methylation, and amplification with both the (M) and (U) primers reveals partial methylation. The amplicon band size for the Unmethylated (U) CDKN2A is 152 bp and methylated (M) c-Myc is 116 bp.

Table 1

Primer sequence, product size and accession number for methylation-specific PCR for target genes

Genes	Primer 5'-3' (Forward)	Primer 5'-3' (reverse)	Product size	Accession number
c-Myc (M)	GTTTCGTTTTTGGTTTAGTTTTTC	TATAAATTCCAATACAAAATACCCG	116	NG_007161
c-Myc (U)	GGTTTTGTTTTTGGTTTAGTTTTTT	ATTCCAATACAAAATACCCACC	112	NG_007161
CDKN2A (M)	GATATTTTTTTAGTCGTATAGGTGATTTC	TTCCTAACTACCAAATTAAATCGAA	150	X94154
CDKN2A (U)	GGATATTTTTTTAGTTGTATAGGTGATTTT	CTTCCTAACTACCAAATTAAATCAAA	152	X94154

M: Methylation PCR primers; U Unmethylation PCR primers

Table 2

Drug docking of estrogen receptor (3ERT) and PIWIL-1 (2L5C)

Compounds	3ERT					PIWIL1				
	Binding energy				Interacted amino acid	Binding energy				Interacted amino acid
	E	VDW	HB	Elec.	(type of bond)	E	VDW	HB	Elec.	(type of bond)
Betulinic acid	-79.14	-72.88	-6.25	0	Tyr526 (HB)	-85.59	-63.8	-18.22	-3.57	Asp320, Arg370, Gly378(HB)
Coumarin	-67.35	-58.82	-8.53	0	Ser468 (HB) Asp374 (PA) Phe461,Leu462,Lys467 (AB)	-69.37	-60.87	-8.5	0	Lys315(HB) Ala335,Tyr345(AB)
Tryptanthrin	-87.39	-77.19	-10.2	0	Lys449,Gly390(HB) Glu323,Arg394,Glu353 (VDW) Pro324 (PS), Ile326,Met357,Leu387(AB)	-77.09	-68.05	-9.04	0	Arg368,Met381(HB) Ala335,Pro379,Ala380 (AB)
Artemisinin	-87.13	-70.27	-16.86	0	Gly390, Lys 449(HB) Pro324(AB)	-82.78	-52.34	-30.44	0	Tyr350(HB) Ty335,Tyr345, Ala380(AB)
Acacetin	-82.41	-64.59	-17.82	0	Ala307,Ser317,Gly366,Asp369,Phe367 (HB) Leu310,Ala318, Pro365(AB)	-76.75	-51.59	-22.11	-3.05	Asp321,Ile322 (HB) Asp321,Trp324(VDW) Lys301,Ile304(AB)
Ferulic Acid	-69.06	-54	-13.97	-1.1	Arg363,Asp369(HB) Pro365 (PS), Gly366 (PD), Als307,Leu310,Val368(AB)	-85.02	-76.14	-17.88	0	Thr316,Arg318, Arg368(HB) Lys315,Lys367(AB)
Calcitriol	-78.08	-64.74	-13.33	0	Asn455,Arg515, Ser456(HB) Ile451,Ile452,Leu508,leu511(AB)	-81.74	-74.37	-7.36	0	Asp269,Arg275,Asp356 (HB) His271,Phe284(AB)

HB: hydrogen bond, AB: alkyl bond, VDW: Van der Waals, PA: pi-anion bond, PS: pi-sigma bond, PD: pi-donor HB

Table 3: Molecular docking between Kaiso (6df5), estrogen receptor (3ERT) and PIWIL1 (2l5c)

Protein-protein interaction (PPI)	Residues or nucleotide in P1	Residues in P2	RMSD (Å)
Kaiso (6df5) (P1) vs PIWIL1 (2l5c) (P2)	**Pose 0.** (chain D: DG9 DC10 DC11 DA12 DA13 DA15 & chain E: DT21 DA23 DT24 DT25 DG26 DA29 DT5 DC6 DC7 DT8 DG9 DG30 DA32 **Pose 1.** (chain D: DT1 DG2 DC3 DT4 DT5 DC6 DC7 DT8 DG9) (chain E: DG30 DA32 DC35 DA36) **Pose 2.** (chain A: DG9 DC10 DC11 DA12 DA13 DT14) (chain E: DG20 DT22 DA23 DA29 DG30)	**Pose 0.** V307 N313 N314 T316 Y317 K334 A335 D336 G337 S338 E339 Y345 Y350 K367 R369 **R370** G371 P379 A380 **M381** T390 L392 M396 R397 N398 **Pose 1.** K311 Y312 N313 N314 T316 Y317 D336 Y345 K348 Q349 Y350 N351 Q352 P366 K367 R368 R369 **R370** G371 P372 G373 **Pose 2.** Y312 N313 N314 K315 T316 Y345 R347 K348 Q349 Y350 N351 R368 **R369 P372**	**4.75**
Kaiso (6df5) (P1) vs 3ERT (P2)	**Pose 0.** (R501 Y503 S508 I515 & (nt chain D) DT1 DG2 DC3 DT4 DT5 DC7 DT8&(nt chain E) DA33 DG34 DC35 DA35) **Pose 1.** (chain A: V504 C505 S508) (nt chain D: DG9 DC10 DG18), (nt chain E: DC19 DG20 DT21 DT22) DG18 DC19 DG20 DT21 DT22 DA23 **Pose 2.** chain A (Q596), chain D (DT8 DC10 DA12 DA13), chain E (DT22 DA23 DT24 DT25 DG27 DA29 DG30)	**Pose 0.** (E380 G457 V458 Y459 T460 **N519 M522 Y526 C530 K531** Y537 G457 V458 Y459 N519 M522) **Pose 1.** R412 K416 M421 V422 D426 M427 G457 V458 Y459 **N519 M522** **Pose 2.** S329 E330 Y331 D332 P333 D351 R352 V355 **C530 K531 V533 V534 P535** D538 L539 M543	**5.05**

RMSD: root-mean-square deviation, Å: Angstrom

4. Discussion

The effect of the naturally occurring BA in the treatment of cancer has been investigated before, however, molecular targets and mechanisms leading to such effect remain mostly unexplored. A previous study indicated the hormonal modulating action of BA via suppressing the ER signalling by reducing ERα mRNA and protein levels [31]. Meanwhile, none reported its potential ability to target amino acid residues within the active binding sites of ER or PIWIL1 polypeptides or investigated its role on the expression of Kaiso or the epigenetic alterations of c-Myc and CDKN2A genes.

The current report aimed to screen and select a potential natural inhibitor for ERα and PIWIL1 proteins via *in silico* molecular docking analysis. The effect of the selected compound which turned to be BA on KAISO mRNA levels, the methylation status of its downstream genes c-Myc and CDKN2A, cell cycle arrest, apoptosis or necrosis induction, and cytotoxicity was investigated.

The in-silico study suggests that BA could block the active binding sites of ERα and PIWIL1 efficiently after binding to Tyr526 in ERα with a short distance of 2.71 Å and low binding energy -79.14 Kcal/Mol, as well as binding to Arg370 and Gly378 in PIWIL1 with the lowest binding energy -85.59 Kcal/Mol. These residues play a crucial role in the regulation of ERα and PIWIL1 functions [32, 33]. This possible binding raises the possibility of a novel anticancer mechanism in which BA disrupts the ER and PIWIL1 signalling, inhibiting tumor progression.

In this aspect, it has been shown that the amino acid residues between 515 and 535 at the C terminus of the human ER are critical for proper interaction with response elements in target genes, and hence play a critical role in its transcriptional activity. Different reports have also shown that phosphorylation at Serine and Tyrosine residues within the ER plays an important role in promoting receptor recycling between the cytoplasm and the nucleus, activation of heterodimerization, cell cycle regulation, and target gene transcription [34, 35]. As per our results, the binding of BA to Tyr526 may interfere with the activation of ligand action and the stimulation of ER dimerization. A previous study indicated the importance of post-translational methylation at Arginine residues by type I and type II of protein methyltransferases to the binding activity of PIWIL1. Particularly, the 9-aa segment, (amino acids residues 370–378) directed the methyl group into the binding site of the PIWIL pocket [36, 37].

Based on the preliminary *in silico* data, we conducted an *in vitro* study to assess the effect of BA on the regulation of Kaiso, one of ER downstream genes, since a previous study discovered that the loss of ER upregulated Kaiso expression [38]. The function of Kaiso as an oncogene or a tumor suppressor is still highly ambiguous. In the current work, a substantial dose-dependent increase in Kaiso expression was observed in MCF-7 (14-fold) and MDA-MB-231 (9-fold) after BA treatment. According to one theory, the anti-neoplastic effects of etoposides are caused by to the overexpression of Kaiso in cells expressing p53 [39].

Our data, therefore, support the tumor suppressor function of Kaiso, particularly given that Kaiso overexpression occurred concurrently with BA's induction of apoptosis and cytotoxicity. The suggestions that Kaiso may function as both a transcription activator and repressor may be dependent on the target with which it interacts; for example, Kaiso's interaction with wild-type p53 activates transcription of pro-apoptotic genes, whereas its interaction with mutant p53 represses transcription of pro-apoptotic genes. Thus, the pro-apoptotic response of MCF-7 cells to KAISO overexpression might be explained by the presence of a wild-type functioning p53; in contrast, wild-type p53 is lost in MDA-MB-231 cells [40] which might explain the balanced apoptosis/necrosis observed in our study rather than the apoptosis as an exclusive mode of cell death.

The effect of BA on epigenetic gene expression was rarely investigated, a single study reported that BA treatment caused a suppression in ERβ expression through epigenetic modification of its promoter in endometriotic cells [41]. To investigate if alteration of cellular epigenetics might contribute to the antitumor activity of BA, we examined the methylation status of the promoter region of two target genes in the Kaiso signaling pathway, a known oncogene; c-Myc, and a tumor suppressor gene; CDKN2A. The inhibitory effect of BA on c-Myc expression was previously reported in several reports [42-44]. On the other hand, hypomethylation of oncogenes such as c-Myc has been suggested to

contribute to its over-expression leading to cancer development [45]. On the other hand, hypomethylation of oncogenes such as c-Myc has been suggested to contribute to its over-expression leading to cancer development [46].

Overall, our epigenetic analysis points to the epigenetic modulatory action of BA through selective promoter methylation, therefore silencing the c-Myc while enhancing the demethylation of the tumor suppressor CDKN2A promoter region, leading to its increased expression in both cell lines, resulting in cell cycle arrest and ultimately leading to cell death.

On the cellular level, our study showed that BA exhibited a concentration-dependent reduction in cell viability accompanied by morphological changes in both MCF-7 and MDA-MB-231 cells, however, the ER (+) MCF-7 cells were more sensitive as evidenced by the 5 folds higher IC_{50} value of BA in MDA-MB-231 (100 µM) compared to that of MCF-7 cells (21 µM). These results support the theory that, in contrast to the ER-deficient MDA-MB-231 cells, BA's main mechanism of action may include binding to the active site of ER in the ER (+) MCF-7 breast cancer cells. Flow cytometer cell cycle analysis revealed a significant G0/G1 arrest after BA treatment, which is consistent with earlier studies conducted on various cell lines, emphasizing the ability of BA to arrest cells in the G0/G1 phase [47]. This is in line with the findings of Foo, et al., who reported a G0/G1 arrest was responsible for BA's anti-proliferative and pro-apoptotic actions in MCF-7 cells [48]. One explanation for the G0/G1 cell cycle arrest and the subsequent apoptosis may be due to BA's ability to induce early DNA damage via direct binding to and inhibition of DNA topoisomerase II in a dose-dependent manner [49].

Evading apoptosis is a fundamental hallmark of cancer cells [50]. Therefore, combating aggressive chemo-therapeutic-resistant cancers like ER (-) cells through targeting both apoptosis and an alternative cell death mechanism such as necroptosis could be adopted for the treatment of such cancers, indeed several studies are reporting on the concept of harnessing necroptosis for fighting aggressive cancers including triple-negative breast cancers with necroptosis-inducing agents [51-54].

In agreement with the cell cycle arrest and morphology results, BA treatment has induced apoptosis in a dose-dependent in MCF-7 but not necrotic cells even at the low, 10% IC_{50} dose. As to be expected, MDA-MB-231 cells were more resistant at low BA dose and responded relatively differently, only treatment with the high, IC_{50} dose (100 µM) caused a significant increase in both apoptotic and necrotic cells.

These data also explain the greater susceptibility of MCF-7 cells to lower doses of BA compared to MDA-MB-231 cells that were only affected using high doses which shifted the cell death mechanism from solely apoptosis to a co-existing necroptosis and apoptosis. Therefore, our findings support the trend of MDA-MB-231 in displaying resistance to anti-cancer agents probably due to its ability to evade apoptosis and perform cell recovery “anastasis” therefore, regaining viability and proliferation capabilities [55].

As mentioned earlier, the preliminary *in silico* study identified the most efficient anti-ERα and anti-PIWIL1 candidate drug; Betulinic acid. Additionally, we explored whether BA can exert an indirect anti-carcinogenic effect on breast cancer cells via the upregulation of KAISO. The molecular docking data showed that KAISO can bind to ER and PIWIL1 with high efficiency at crucial residues, in turn, it can block their signal pathway. We suggest that KAISO can bind to ER with many bonds especially, tyrosine residues including (Y526 and Y537), Methionine (Met421), and cysteine (C530). Many previous studies reported the essential role of Y537 in the binding with Estrogen, binding to response elements in target genes, and transcription activation [56]. Also, it has been demonstrated that C530 is the main residue at the binding site with Estrogen and Tamoxifen [57]. Moreover, Methionine (Met421) is a crucial residue in the binding cavity [58]. In addition, we show that KAISO may bind to PIWIL1 through multiple bonds at many residues within the loop extended from 369 to 378 including R369 R370 P372 that play an important role in the destination of a methyl group at the 3′ end for further loading in the binding pocket. Also, many nucleotides of KAISO bind to M381 which is essential for binding the 2'-O-methylated 3'-end of piRNAs [33].

5. Conclusions

We conclude that the hormonal modulating and cytotoxicity actions of BA might be attributed to its ability to block the ERα and PIWIL1 signaling pathways and so on of its target gene; Kaiso gene expression and selective alterations in the

methylation status of the c-Myc and CDKN2A genes leading to cell cycle arrest and ultimately cell death. BA proved to be effective against both ER (+) cells by inducing apoptosis and ER (-) cells by shifting towards necroptosis, such data might undoubtedly provide a potential clinical benefit for BA, including the treatment of triple negative breast cancer.

6. Conflicts of interest

There are no conflicts to declare.

7. Formatting of funding sources

No funding was received from any organization for conducting this study.

8. References

[1] Kashyap D, Pal D, Sharma R, Garg VK, Goel N, Koundal D, Zaguia A, Koundal S, Belay A. Global Increase in Breast Cancer Incidence: Risk Factors and Preventive Measures. Biomed Res Int.2022;2022:9605439.

[2] Karami Fath M, Azargoonjahromi A, Kiani A, Jalalifar F, Osati P, Akbari Oryani M, Shakeri F, Nasirzadeh F, Khalesi B, Nabi-Afjadi M, Zalpoor H, Mard-Soltani M, Pavandeh Z. The role of epigenetic modifications in drug resistance and treatment of breast cancer. Cell Mol Biol Lett. 2022;27(1):52.

[3] Sleightholm R, Neilsen BK, Elkhatib S, Flores L, Dukkipati S, Zhao R, Choudhury S, Gardner B, Carmichael J, Smith L, Bennion N, Wahl A, Baine M. Percentage of hormone receptor positivity in breast cancer provides prognostic value: a single-institute study. Journal of clinical medicine research 2021;131: 9.

[4] Cecilia W and Lin CY. Oestrogen receptors in breast cancer: basic mechanisms and clinical implications. Ecancermedicalscience 2013; 7.

[5] Sharma D, Kumar S, Narasimhan B. Estrogen alpha receptor antagonists for the treatment of breast cancer: a review. Chemistry Central Journal 2018; 12: 1-32.

[6] Yao J, Deng K, Huang J, Zeng R, Zuo J. Progress in the understanding of the mechanism of tamoxifen resistance in breast cancer. Frontiers in Pharmacology 2020;11: 592912.

[7] Dong P, Xiong Y, Konno Y, Ihira K, Xu D, Kobayashi N, Yue J, Watari H. Critical Roles of PIWIL1 in Human Tumors: Expression, Functions, Mechanisms, and Potential Clinical Implications. Frontiers in Cell and Developmental Biology 2021;9: 656993.

[8] Pan Y, Hu M, Liang H, Wang JJ, Tang LJ. The expression of the PIWI family members miwi and mili in mice testis is negatively affected by estrogen. Cell and tissue research 2012;350(1): 177-181.

[9] Zhang D, Duarte-Guterman P, Langlois VS, Trudeau VL. Temporal expression and steroidal regulation of piRNA pathway genes (mael, piwi, vasa) during Silurana (Xenopus) tropicalis embryogenesis and early larval development. Comparative Biochemistry and Physiology Part C: Toxicology & Pharmacology 2010;152(2): 202-206.

[10] Chen Z, Che Q, He X, Wang F, Wang H, Zhu M, Sun J, Wan X. Stem cell protein Piwil1 endowed endometrial cancer cells with stem-like properties via inducing epithelial-mesenchymal transition. BMC cancer 2015;15(1):1-13.

[11] Pierre CC, Hercules SM, Yates C, Daniel JM. Dancing from bottoms up–roles of the POZ-ZF transcription factor Kaiso in cancer. Biochimica et Biophysica Acta (BBA)-Reviews on Cancer 2019; 1871;(1): 64-74.

[12] Lopes EC, Valls E, Figueroa ME, Mazur A, Meng FG, Chiosis G, Laird PW, Schreiber-Agus N, Greally JM, Prokhortchouk E, Melnick A. Kaiso contributes to DNA methylation-dependent silencing of tumor suppressor genes in colon cancer cell lines. Cancer research 2008; 68 (18): 7258-7263.

[13] Koh DI, Yoon JH, Kim MK, An H, Kim MY, Hur MW. Kaiso is a key regulator of spleen germinal center formation by repressing Bcl6 expression in splenocytes. Biochemical and Biophysical Research Communications 2013; 442(3-4): 177-182.

[14] Prokhortchouk A, Hendrich B, Jørgensen H, Ruzov A, Wilm M, Georgiev G, Bird A, Prokhortchouk E. The p120 catenin partner Kaiso is a DNA methylation-dependent transcriptional repressor. Genes & development 2001;15(13):1613-1618.

[15] Cofre J, Menezes JR, Pizzatti L, Abdelhay E. Knock-down of Kaiso induces proliferation and blocks granulocytic differentiation in blast crisis of chronic myeloid leukemia. Cancer cell international 2012;12(1): 1-14.

[16] Qin S, Zhang B, Tian W, Gu L, Lu Z, Deng D. Kaiso mainly locates in the nucleus in vivo and binds to methylated, but not hydroxymethylated DNA. Chinese Journal of Cancer Research 2015; 27(2): 148.

[17] Akervall J, Bockmühl U, Petersen I, Yang K, Carey TE, Kurnit DM. The gene ratios c-MYC: cyclin-dependent kinase (CDK) N2A and CCND1: CDKN2A correlate with poor prognosis in squamous cell carcinoma of the head and neck. Clinical cancer research 2003;9(5): 1750-1755.

[18] Kaplun D, Starshin A, Sharko F, Gainova K, Filonova G, Zhigalova N, Mazur A, Prokhortchouk E, Zhenilo S. Kaiso regulates DNA methylation homeostasis. International journal of molecular sciences 2021; 22(14): 7587.

[19] Carlos-Reyes Á, López-González JS, Meneses-Flores M, Gallardo-Rincón D, Ruíz-García E, Marchat LA, Astudillo-de la Vega H, Hernández de la Cruz ON, López-Camarillo C. Dietary compounds as epigenetic modulating agents in cancer. Frontiers in genetics 2019;10: 79.

[20] Singh S, Gupta P, Meena A, Luqman S. Acacetin, a flavone with diverse therapeutic potential in cancer, inflammation, infections and other metabolic disorders. Food and Chemical Toxicology 2020;145: 111708.

[21] Wu Y, Xu J, Liu Y, Zeng Y, Wu G. A review on anti-tumor mechanisms of coumarins. Frontiers in Oncology 2020; 10: 2720.

[22] Zeng Q, Luo C, Cho J, Lai D, Shen X, Zhang X, Zhou W. Tryptanthrin exerts anti-breast cancer effects both in vitro and in vivo through modulating the inflammatory tumor microenvironment. Acta Pharmaceutica 2021;71(2): 245-266.

[23] Augustin Y, Staines HM, Krishna S. Artemisinins as a novel anti-cancer therapy: targeting a global cancer pandemic through drug repurposing. Pharmacology & Therapeutics 2020: 216: 107706.

[24] Zhang X, Lin D, Jiang R, Li H, Wan J, Li H. Ferulic acid exerts antitumor activity and inhibits metastasis in breast cancer cells by regulating epithelial to mesenchymal transition. Oncology Reports 2016; 36(1): 271-278. (2016)

[25] Swami S, Krishnan AV, Wang JY, Jensen K, Peng L, Albertelli MA, Feldman D. Inhibitory effects of calcitriol on the growth of MCF-7 breast cancer xenografts in nude mice: selective modulation of aromatase expression in vivo. Hormones and Cancer 2011;2(3): 190-202.

[26] Qi X, Gao C, Yin C, Fan J, Wu X, Guo C. Improved anticancer activity of betulinic acid on breast cancer through a grafted copolymer-based micelles system. Drug delivery 2021;28(1): 1962-1971.

[27] Lou H, Li H, Zhang S, Lu H, Chen Q. A review on preparation of betulinic acid and its biological activities. Molecules 2021;26(18): 5583.

[28] Riss TL, Moravec RA, Niles AL, Duellman S, Benink HA, Worzella TJ, Minor L. Cell Viability Assays. 2013 May 1 [updated 2016 Jul 1]. In: Markossian S, Grossman A, Brimacombe K, Arkin M, Auld D, Austin C, Baell J, Chung TDY, Coussens NP, Dahlin JL, Devanarayan V, Foley TL, Glicksman M, Haas JV, Hall MD, Hoare S, Inglese J, Iversen PW, Kales SC, Lal-Nag M, Li Z, McGee J, McManus O, Riss T, Saradjian P, Sittampalam GS, Tarselli M, Trask OJ Jr, Wang Y, Weidner JR, Wildey MJ, Wilson K, Xia M, Xu X, editors. Assay Guidance Manual [Internet]. Bethesda (MD): Eli Lilly & Company and the National Center for Advancing Translational Sciences; 2004–. PMID: 23805433.

[29] Wlodkowic D, Skommer J, Darzynkiewicz Z. Flow cytometry-based apoptosis detection. In apoptosis, pp. 19-32. Humana Press, Totowa, NJ, (2009).

[30] Li LC, Dahiya R. MethPrimer: designing primers for methylation PCRs. Bioinformatics 2002;18(11): 1427-1431.

[31] Kim HJ, Quan FS, Kim JE, Lee NR, Kim HJ, Jo SJ, Lee CM, Jang DS, Inn KS. Inhibition of estrogen signaling through depletion of estrogen receptor alpha by ursolic acid and betulinic acid from Prunella vulgaris var. lilacina. Biochemical and biophysical research communications 2014;451(2): 282-287.

[32] Rollerova E and Urbancikova M. Intracellular estrogen receptors, their characterization and function. Endocr Regul 2000;34(4): 203-218.

[33] Yuan T, Simanshu DK, Ma JB, and Patel DJ. Structural basis for piRNA 2'-O-methylated 3'-end recognition by Piwi PAZ (Piwi/Argonaute/Zwille) domains. Proceedings of the National Academy of Sciences 2011; 108(3): 903-910.

[34] de Leeuw R, Neefjes J, Michalides R. A role for estrogen receptor phosphorylation in the resistance to tamoxifen. Int J Breast Cancer. 2011;2011:232435. doi: 10.4061/2011/232435.

[35] Helzer KT, Szatkowski Ozers M, Meyer MB, Benkusky NA, Solodin N, Reese RM, Warren CL, Pike JW, Alarid ET. The phosphorylated estrogen receptor α (ER) cistrome identifies a subset of active enhancers enriched for direct ER-DNA binding and the transcription factor GRHL2. Molecular and cellular biology 2019;39(3): e00417-18.

[36] Castoria G, Giovannelli P, Lombardi M, De Rosa C, Giraldi T, de Falco A, Barone MV, Abbondanza C, Migliaccio A, Auricchio F. Tyrosine phosphorylation of estradiol receptor by Src regulates its hormone-dependent nuclear export and cell cycle progression in breast cancer cells. Oncogene 2012;31(46): 4868-4877.

[37] Yohei K, Kim N, de Planell-Saguer M , Khandros E, Chiorean S, Klein PS, Rigoutsos I, Jongens TA, and Mourelatos Z. Arginine methylation of Piwi proteins catalysed by dPRMT5 is required for Ago3 and Aub stability. Nature cell biology 2009; 11(5): 652-658.

[38] Vagin VV, Wohlschlegel J, Qu J, Jonsson Z, Huang X, Chuma S, Girard A, Sachidanandam R, Hannon GJ, Aravin AA. Proteomic analysis of murine Piwi proteins reveals a role for arginine methylation in specifying interaction with Tudor family members. Genes & development 2009;23(15): 1749-1762.

[39] Bassey-Archibong BI, Rayner LG, Hercules SM, Aarts CW, Dvorkin-Gheva A, Bramson JL, Hassell JA, Daniel JM. Kaiso depletion attenuates the growth and survival of triple negative breast cancer cells. Cell death & disease 2017;8(3): e2689-e2689.

[40] Hui L, Zheng Y, Yan Y, Bargonetti J and Foster DA. Mutant p53 in MDA-MB-231 breast cancer cells is stabilized by elevated phospholipase D activity and contributes to survival signals generated by phospholipase D. Oncogene 2006;25(55):7305-7310.

[41] Xiang D, Zhao M, Cai X, Wang Y, Zhang L, Yao H, Liu M, Yang H, Xu M, Li H, Peng H, Wang M, Liang X, Li L, Yao P. Betulinic Acid Inhibits Endometriosis Through Suppression of Estrogen Receptor β Signaling Pathway. Frontiers in endocrinology 2020;11: 604648.

[42] Zheng Y, Liu P, Wang N, Wang S, Yang B, Li M, Chen J, Situ H, Xie M, Lin Y, Wang Z. Betulinic Acid Suppresses Breast Cancer Metastasis by Targeting GRP78-Mediated Glycolysis and ER Stress Apoptotic Pathway. Oxid Med Cell Longev. 2019;19:8781690.

[43] Hao Z, Mu X, Zhang X, and You Q. Lung cancer inhibition by betulinic acid nanoparticles via adenosine 5′-triphosphate (ATP)-binding cassette transporter G1 gene downregulation. Medical Science Monitor: International Medical Journal of Experimental and Clinical Research 2020;26: e922092-1.

[44] Justyna K, Strzadala L, and Rapak A. Sorafenib in combination with betulinic acid synergistically induces cell cycle arrest and inhibits clonogenic activity in pancreatic ductal adenocarcinoma cells. International Journal of Molecular Sciences 2018;19(10): 3234.

[45] Spitzwieser M, Entfellner E, Werner B, Pulverer W, Pfeiler G, Hacker S, Cichna-Markl M. Hypermethylation of CDKN2A exon 2 in tumor, tumor-adjacent and tumor-distant tissues from breast cancer patients." BMC cancer 2017;17(1): 1-16.

[46] Parris TZ, Kovács A, Hajizadeh S, Nemes S, Semaan M, Levin M, Karlsson P, Helou K. Frequent MYC coamplification and DNA hypomethylation of multiple genes on 8q in 8p11-p12-amplified breast carcinomas. Oncogenesis 2014;3(3): e95-e95.

[47] Mullauer, Franziska B., Jan H. Kessler, and Jan Paul Medema. "Betulinic acid induces cytochrome c release and apoptosis in a Bax/Bak-independent, permeability transition pore dependent fashion." Apoptosis 2009;14(2): 191-202.

[48] Foo JB, Saiful Yazan L, Tor YS, Wibowo A, Ismail N, How CW, Armania N, Loh SP, Ismail IS, Cheah YK, Abdullah R. Induction of cell cycle arrest and apoptosis by betulinic acid-rich fraction from Dillenia suffruticosa root in MCF-7 cells involved p53/p21 and mitochondrial signalling pathway. Journal of ethnopharmacology 2015;166: 270-278.

[49] Wada S, Tanaka R. Betulinic acid and its derivatives, potent DNA topoisomerase II inhibitors, from the bark of Bischofia javanica." Chemistry & biodiversity 2005;2(5): 689-694.

[50] Douglas H. and Weinberg RA. The hallmarks of cancer. cell 2000;100(1): 57-70.

[51] Cho YS, Park SY. Harnessing of programmed necrosis for fighting against cancers. Biomolecules & Therapeutics 2014;22(3): 167.

[52] Gong Y, Fan Z, Luo G, Yang C, Huang Q, Fan K, Cheng H, Jin K, Ni Q, Yu X, Liu C. The role of necroptosis in cancer biology and therapy. Molecular cancer 2019;18(1): 1-17.

[53] Ayaz N, Chen H, and Yuan J. Necroptosis and cancer. Trends in cancer 2017;3(4): 294-301.

[54] Zahra S, Karami-Tehrani F, and Salami S. Targeting cell necroptosis and apoptosis induced by shikonin via receptor interacting protein kinases in estrogen receptor positive breast cancer cell line, MCF-7. Anti-Cancer Agents in Medicinal Chemistry (Formerly Current Medicinal Chemistry-Anti-Cancer Agents) 2018;18(2): 245-254.

[55] Seervi M, Sumi S, Chandrasekharan A, Sharma AK, SanthoshKumar TR. Molecular profiling of anastatic cancer cells: potential role of the nuclear export pathway. Cellular Oncology 2019;42(5): 645-661.

[56] Arnold SF, Vorojeikina DP, Notides AC. Phosphorylation of Tyrosine 537 on the Human Estrogen Receptor Is Required for Binding to an Estrogen Response Element. Journal of Biological Chemistry 1995;270(50): 30205-30212.

[57] Harlow KW, Smith DN, Katzenellenbogen JA, Greene GL and Katzenellenbogen BS. Identification of cysteine 530 as the covalent attachment site of an affinity-labeling estrogen (ketononestrol aziridine) and antiestrogen (tamoxifen aziridine) in the human estrogen receptor. Journal of Biological Chemistry 1989;264(29): 17476-17485.

[58] Bhat RA, Stauffer B, Unwalla RJ, Xu Z, Harris HA, Komm BS. Molecular determinants of ERα and ERβ involved in selectivity of 16α-iodo-17β estradiol. The Journal of Steroid Biochemistry and Molecular Biology 2004;88(1): 17-26.